LWT - Food Science and Technology 125 (2020) 109250

Contents lists available at ScienceDirect

LWT - Food Science and Technology

journal homepage: www.elsevier.com/locate/lwt

Rapid detection of pure coconut oil adulteration with fried coconut oil using ATR-FTIR spectroscopy coupled with multivariate regression modelling

Amit[a,1], Rahul Jamwal[a,1], Shivani Kumari[a], Simon Kelly[b], Andrew Cannavan[c], Dileep Kumar Singh[a,*]

[a] Soil Microbial Ecology and Environmental Toxicology Laboratory, Department of Zoology, University of Delhi, New Delhi, Delhi, 110007, India
[b] Food and Environmental Protection Laboratory, International Atomic Energy Agency, Vienna International Centre, PO Box 100, 1400, Vienna, Austria
[c] Seibersdorf Laboratory, International Atomic Energy Agency, Vienna International Centre, PO Box 100, 1400, Vienna, Austria

ARTICLE INFO

Keywords:
FTIR
Adulteration
Fried coconut oil
Regression modelling
Multivariate

ABSTRACT

Attenuated total reflection- Fourier transform infrared (ATR-FTIR) spectroscopy along with multivariate regression modelling was utilized to develop the methodology for classification and quantification of refined, bleached and deodorized (RBD) pure coconut oil (PCO) from its adulterant RBD fried coconut oil (FCO). Principal component analysis (PCA) was applied on 3000-2800 cm^{-1}, and 1800-500 cm^{-1} and linear discriminant analysis (LDA) was used on selected 13 wavenumbers. Principal components regression (PCR) and Partial least squares regression (PLS-R) models were constructed and compared for normal, 1st, and 2nd derivatives. PLS-R model for the 1st derivative of 1800-500 cm^{-1} showed the best results for prediction with high precision and accuracy (RPD: 20.03, RE %: 4.288). The lowest limit of detection of FCO in PCO was predicted as 0.5% v/v. This detected concentration is not the constraint of the experiment pursued; instead, it is the lowest concentration of FCO adulteration used in our work. Our findings are only applicable to detection of FCO adulteration at same frying degree while adulteration detection of FCO at different frying degrees is altogether a different adulteration issue. This study provides valuable information to oil industries and the regulatory authorities to build standard guidelines for the detection of oil adulteration.

1. Introduction

Edible oils are an integral part of our diet because they supply energy, vitamins, and essential fatty acids vital for the healthy development of our body. In addition to providing nutrition, they also act as functional oil for food preparation leading to the temptation of processed foods. The edible oils which are used at the time of deep frying lead to the deterioration process, making it one of the critical aspects of fried food products. Refined, bleached, and deodorized (RBD) coconut oil is extensively used for baking, cooking, and deep drying purposes remarkably in South India and Southeast Asian countries (Ghani et al., 2018; Marina, Man, & Amin, 2009). Uncooked RBD coconut oil retains its entire nutritional constituents like vitamin E, pro-vitamin A, antioxidants, and essential fatty acids.

Globally, deep-frying is one of the prominent methods for food preparation. At the time of frying, RBD coconut oil is heated up to 170–180 °C for an extended period and are exposed to both oxygen and moisture supply (Guillaume, De Alzaa, & Ravetti, 2018; Koh & Long, 2012). Due to high temperature, while frying, oil inescapably undergoes a series of chemical transformations, including lipid hydrolysis, oxidation, polymerization, cyclization, and isomerization, which will produce adverse effects and even generates toxic compounds like heterocyclic amines (Brühl, 2014). At the time of frying, there is a considerable change in color and viscosity of the oil, and it gets an obnoxious taste and aroma (Ghobadi, Akhlaghi, Shams, & Mazloomi, 2018; Sunisa, Worapong, Sunisa, Saowaluck, & Saowakon, 2011). Therefore, during every frying process, fried coconut oil (FCO) is suggested to be replaced with pure and fresh coconut oil (PCO) to avoid deterioration. But for lucrative purposes, this practice is usually avoided by street food vendors, and the leftover fried and deteriorated coconut oil is blended with pure coconut oil for further cooking and frying. This wrong practice of reusing heated coconut oil creates severe public health complications such as high blood pressure and a considerable increase in inflammatory biomarkers (Hamsi et al., 2015).

Analysis of coconut oil quality is of deep concern but has not been the subject of research in the recent past. However, many chemical

* Corresponding author.
E-mail address: dileepksingh@gmail.com (D.K. Singh).
[1] Amit and Rahul Jamwal have equal contribution and should be treated as first authors.

https://doi.org/10.1016/j.lwt.2020.109250
Received 22 October 2019; Received in revised form 4 February 2020; Accepted 5 March 2020
Available online 07 March 2020
0023-6438/

Abbreviations

ATR	Attenuated Total Reflectance
FTIR	Fourier Transform Infrared
GC	Gas Chromatography
PCO	Pure Coconut Oil
FCO	Fried Coconut Oil
PCA	Principal Component Analysis
LDA	Linear Discriminant Analysis
PCR	Principal Component Regression
PLS-R:	Partial Least Square Regression
R^2	Coefficient of determination
RBD	Refined, bleached and deodorized
RPD	Residual Predictive Deviation
RE %	Relative Prediction Error
RMSEC	Root Mean Square Error of Calibration
RMSECV	Root Mean Square Error of Cross-Validation
RMSEP	Root Mean Square Error of Prediction
SNV	Standard Normal Variate

parameters such as total polar compounds, peroxide values, carbonyl value, different glycerides, and p-anisidine values have been frequently used to determine the quality of coconut oil (Endo, 2018; Hammouda, Zribi, Mansour, Matthäus, & Bouaziz, 2017; Zribi, Jabeur, Flamini, & Bouaziz, 2016). Nonetheless, most of these methods have the drawback of being destructive, tedious, time taking and unstable for the online monitoring process. Therefore, the development of precise, inexpensive, and rapid methodology of coconut frying oil deterioration analysis is needful in the food market. Attenuated total reflection-Fourier transform infrared (ATR-FTIR) spectroscopy is an immensely stable and responsive approach for quantification of fats and edible oil blending (Amit et al., 2020). It is an abrupt, non-fatal method with the least sample readiness. Previously, oxidation stability of frying of RBD coconut oil has been studied by utilizing Gas Chromatography showing no major change in the fatty acid profile (Koh & Long, 2012). And in another case, oxidative stability of coconut oil has been studied using FTIR spectroscopy. Still, this study only showed peak changes as an effect of oxidation during storage, but it was not precise and lacked a quantitative analysis of FCO (Moigradean, Poiana, & Gogoasa, 2012). Besides this, there is no prominent report regarding the detection of FCO adulteration in PCO using ATR-FTIR spectroscopy along with regression modelling. In our study, we have detected adulteration of PCO with different concentration of FCO at same degree of frying while adulteration detection of FCO at different frying degrees is altogether a different adulteration issue, which is not addressed in our case. Multivariate chemometrics has been vastly employed to examine the FTIR spectral data in the recent past (Jamwal et al., 2020; Varmuza & Filzmoser, 2016). In this case, we have been able to develop a vigorous method for the quantification of PCO adulteration with FCO.

2. Material and methods

2.1. Methodology adopted

The present study aimed to differentiate and detect the lowest limit of FCO in PCO using ATR-FTIR spectroscopy coupled with multivariate regression modelling. Initially, PCA and LDA have been used to differentiate and classify binary mixture of FCO and PCO. Further, PCR and PLS-R regression models have been applied on the combined optimized region (3000-2800 cm^{-1} and 1800-500 cm^{-1}) as well as for the two separate optimized regions 3000-2800 cm^{-1} and 1800-500 cm^{-1} respectively and compared for normal, 1st and 2nd derivatives to build a vigorous method for the quantification of PCO adulteration with FCO. The optimization process was performed by choosing particular spectral regions containing the extremely valuable variables which are corresponded to the major absorbance bands demonstrating leading attributes of the oil under analysis.

2.2. Sample collection

RBD coconut oil (Patanjali®) was procured from the local supermarket in New Delhi, India.

2.3. Frying experiment

Frying of PCO was executed by adopting the methodology devised by Y.B. Che Man and C.P. Tan in 1999 (Che Man & Tan, 1999). First of all, raw and fresh potatoes were peeled off and cut into a thickness of 2 mm. And to avoid browning, slices were stored in 0.1% (w/v) sodium chloride solution. At the time of frying, these potato slices were slightly dried using tissue paper and weighed in batches of 100 g each. A total of 4.5 Kg of PCO was poured into a batch fryer for the frying experiment. The temperature was raised to 180 °C and maintained for the first 20 min before frying. A batch of 100 g potato slices was fried for 2.5 min at an interval of 17.5 min for 3.5 h per day. It is equal to 10 fryings per day for successive seven days. In the course of frying, the fryer was kept uncovered. At the end of the day (10th frying), the fryer was switched off, fryer lid was covered, and oil was left overnight to cool down. The next day, fresh PCO was added, and all the above steps were repeated till the 7th day of frying. A total of 120 g of FCO sample was collected, the temperature was brought to 60 °C and later stored at 4 °C. Samples were analyzed within two weeks of frying.

2.4. Fatty acid composition analysis by Gas Chromatography

The change in fatty acid composition between PCO and FCO was verified as fatty acid methyl esters (FAME) using Gas Chromatography "Shimadzu GC-2010 (Shimadzu Corporation, Tokyo, Japan)", equipped with Flame ionization detector (FID). The methodology adopted for the extraction of FAMEs was, according to Amit et al., (2020), with few changes.

2.5. Adulteration experiment and sample preparation

As presented in Table 1, a total of 12 blends (PCO/FCO) were created as 0.5%, 1%, and then in arithmetic progression with an increment of 5%, up to 50% v/v, achieving a total of 83 samples. Out of these, 70 samples (5 PCO, 5 FCO, and 60 PCO/FCO blend samples) were prepared as "calibration set" to be used for qualitative studies by PCA and

Table 1
Adulteration experiment and sample preparation.

Calibration Set	
PCO[a] branded oil samples	FCO[b] adulterant
(5 replicates for each adulteration level)	Sample of PCO adulterated with FCO 0.5–50% (12 × 5) = 60
Total 5 pure PCO	5 Samples
Total 5 pure FCO	5 Samples
External Set	
(1 replicate for each adulteration level)	Sample of PCO adulterated with FCO 0.5–50% (12 × 1) = 12
Total 1 pure PCO	1 Samples
Grand Total	**70 Calibration set + 13 External set = 83 samples**

[a] PCO: Pure and fresh Coconut Oil.
[b] FCO: Fried Coconut Oil.

LDA as well as to develop calibration models (PCR and PLS-R). And "external set" of 13 samples (1 PCO and 12 PCO/FCO blend samples) were prepared in the same proportions for the developed model prediction. All samples were completely homogenized and stocked at 4 °C till further use.

2.6. FTIR spectra acquisition

For measurement of FTIR spectra in mid-infrared region (4000–400 cm^{-1}), a "A Thermo-Scientific®–Nicolet iS50 FTIR spectrophotometer (Waltham, Massachusetts, USA)" was used, which was fitted with a diamond crystal cell Attenuated total reflection (ATR) accessory, a deuterated triglycine sulphate (DTGS) detector & a KBr (Potassium bromide) beam splitter. All the spectra were measured with data spacing of 0.482 cm^{-1} and a resolution of 4 cm^{-1} with 32 numbers of the scan. The instrument was connected to "OMNIC 9.2.41 software (Thermo scientific)" (https://www.thermofisher.com/order/catalog/product/833-036200) for the spectral analysis. For spectral measurement, 2 μL of the sample was loaded with the help of a Pasteur pipette on the beam splitter, which developed a thin film. The collected spectra were subtracted from the background spectrum, and a new reference spectrum was documented after every three scans.

2.7. Spectral data pre-treatment

Before performing the chemometric analysis, to get rid of the baseline drift and variability in the intensity, obtained spectra were smoothened using "Unscrambler X 10.5.1" (https://www.camo.com/unscrambler/) by employing Savitzky-Golay method having window point of 7 and a 2nd order polynomial (Savitzky & Golay, 1964). For the smoothening purpose, large frame size and low polynomial order are recommended. Besides, other pre-treatments like mean centering coupled with standard normal variate (SNV) was also performed on the spectral data (Jovic, Smolić, Primožič, & Hrenar, 2016; Wójcicki, Khmelinskii, Sikorski, & Sikorska, 2015; Zhang, Saha, & Vishwanathan, 2012). Viscosity differences arise in PCO, and FCO can affect the construction of a robust regression model due to the formation of baseline offset and slope. Therefore, to eliminate the influence of such undesired effects, mathematical transformations such as 1st and 2nd derivatives were applied to extract only the vital information. These derivatives facilitate the visualization of those peaks which are complex to detect in the original spectra. Baseline offsets were removed by the 1st derivative whereas the 2nd derivative eliminates both baseline and slope (Kamruzzaman, Makino, & Oshita, 2016). The entire data was pre-processed using the Savitzky-Golay approach with a gap of 7 points and second-order polynomial fitting (Savitzky & Golay, 1964).

2.8. Statistical analysis using chemometrics

Initially, PCA was applied to the calibration set of combined optimized spectral data (3000-2800 cm^{-1} and 1800-500 cm^{-1}) to analyze the differences among the samples. PCA converts a large number of potentially correlated variables into a lesser number of principal components (PCs), which are not correlated to each other. It leads to an overall decrease in the size of the dataset (Vasconcelos, Coelho, Barros, & de Almeida, 2015). PCA granted the recognition of the most important wavenumbers responsible for the differences between different samples used, and it also eliminates the less informative wavenumbers, making the most robust PCA model. For qualitative analysis, the most informative variables obtained from the PCA loading spectra were then subjected to discriminant analysis for determining the possible outcome of a sample to pertain to a formerly determined cluster. LDA is performed using "IBM SPSS Statistics 20" (https://www.ibm.com/in-en/products/spss-statistics). LDA is a frequently used supervised pattern recognition method that finds an optimal linear projection that maximizes the ratio between-class variance and decreases the ratio of within-class variance. The distance between the classes mean is usually calculated by Euclidean distance methods. Further, the two most general multivariate regression methods PCR and PLS-R were used to develop calibration models for the quantification of adulterants by employing "Unscrambler X 10.5.1 software using a calibration set of data. An external set of samples was used to judge the predictive performance of the calibration model. Both PCR and PLS-R are the most common quantitative spectral decomposition techniques for spectral calibration and prediction (Lim, Abdul Mutalib, Khaza'ai, & Chang, 2018). PLS-R is a quantitative decomposition method that is much related to PCR but differs slightly in how they decompose the data. PCR initially decompose the spectral data matrix into a set of scores and loadings and then regress them against the concentration as a separate step. At the same time, PLS-R uses concentration information during the decomposition process. PCR does not take into account the errors produce in spectra and concentration estimates, but PLS-R does. Often, similar results were produced due to the similarity in these methods. In our study, one combined optimized region (3000-2800 cm^{-1} and 1800-500 cm^{-1}) and two separate optimized regions 3000-2800 cm^{-1} and 1800-500 cm^{-1} were used to build PCR and PLS-R models. Optimization of specific spectral data sets was done based on key wavenumbers showing main spectral peaks, which reflect the important oil characteristics. Optimization process aids in examining a particular spectral data matrix in terms of better relation between spectral data (self-reliant variable "Y") and the various percentages of FCO in PCO (reliant variable "X") by constructing PCR and PLS-R models. (Pereira, Leite, Andrade, Bell, & Anjos, 2019; Rohman, Setyaningrum, & Riyanto, 2014). However, certain regions in the spectra showing low signal to

Table 2
Wavenumbers of bands on FTIR spectra in mid-infrared region, along with the assigned functional groups, vibrational modes and their intensities for PCO (Amit et al., 2020).

Wavenumbers (cm^{-1})	Functional groups	Assignment	Intensities
2954	–C–H (–CH_3)	Stretching (asymmetrical)	Medium
2924	–C–H (–CH_2)	Stretching (asymmetrical)	Very strong
2852	–C–H (–CH_2)	Stretching (symmetrical)	Very strong
1743	–C═O (ester group)	Stretching	Very strong
1465	–C–H (–CH_2, CH_3)	Bending (scissor)	Medium
1417	= C–H (*cis*-)	Bending (rocking)	Weak
1377	–C–H (–CH_3)	Bending (symmetrical)	Medium
1228	–C–O	Stretching	Medium
1155	–C–O	Stretching	Strong
	–CH_2–	Bending	
1111	–C–O	Stretching	Medium
962	–HC═CH– (*trans*-)	Out of plane bending	Weak
872	= CH_2	Bending (wagging)	Weak
721	–(CH_2)*n*–	Bending (rocking)	Medium

noise ratio (SNR) were omitted out of the analysis (Vasconcelos et al., 2015).

The potential of both models was compared based on RMSEC, RMSECV, and R^2 values using the calibration dataset, whereas R^2 and RMSEP values were used to test the predictive ability of the constructed models using an external dataset. The model with higher R^2 (near to 1) and least RMSE and RE % values is considered as most efficient. Besides, the bias (BIAS), standard error of prediction (SEP), and the residual predictive deviation (RPD) values were calculated, which depicts the precision and accuracy of the constructed models (Andrade et al., 2019).

3. Results and discussion

3.1. FTIR spectral analysis

FTIR spectra of PCO in the optimized region demonstrate many well resolved characteristic peaks (bond vibrations) at specific wavenumber (cm^{-1}) that can be assigned to functional groups of its fatty acids, as shown in Table 2 (Amit et al., 2020). As depicted by the FTIR spectra of PCO and its different FCO adulterants (Fig. 1), 3000–2800 cm^{-1} and 1800-500 cm^{-1} are the two major 'informative' regions. Predominantly, 2954 cm^{-1}, 2924 cm^{-1} and 2852 cm^{-1} from 1st informative region and 1743 cm^{-1}, 1465 cm^{-1}, 1417 cm^{-1}, 1377 cm^{-1}, 1228 cm^{-1}, 1155 cm^{-1}, 1111 cm^{-1}, 962 cm^{-1}, 872 cm^{-1} and 721 cm^{-1} from 2nd informative region manifests coherent differences in spectra. These specific wavenumbers are assigned to different functional groups, modes of vibration, and intensities. These differences are attributed to the change in different fatty acid bonds during coconut oil deep frying. Moreover, from the fatty acid analysis by GC (Table 3), there was very little change in the fatty acid profile of PCO during deep frying. During frying, the formation of conjugated dienes is proportional to the linoleic acid content of the oil, and PCO has a lower percentage of polyunsaturated fatty acids, i.e., linoleic acid (Koh & Long, 2012). As a result, due to less formation of conjugated dienes during frying of RBD coconut oil, little changes in the fatty acid profile cannot help in adulteration detection. However, FTIR, along with chemometrics, has many advantages over GC analysis in the detection of FCO adulteration in PCO (Henna Lu & Tan, 2009; Jamwal et al., 2020). It can be observed from the spectra that with the increase in the concentration of FCO, absorbance decreases. But it is difficult to differentiate PCO and its FCO adulterants visually. So, multivariate chemometrics was further applied for the differentiation and detection of FCO adulterants from PCO.

Table 3
Changes in fatty acid (%) profile of pure RDB coconut oil during frying experiment.

Fatty acids (%)	Pure RBD CO[a] (%)	Fried RBD CO (%)
Caproic acid (C6:0)	0.84 ± 0.03	0.62 ± 0.02
Caprylic acid (C8:0)	9.18 ± 0.01	9.11 ± 0.04
Capric acid (C10:0)	6.93 ± 0.05	7.01 ± 0.02
Lauric acid (C12:0)	48.98 ± 0.02	50.08 ± 0.01
Myristic acid (C14:0)	18.24 ± 0.01	17.93 ± 0.05
Palmitic acid (C16:0)	8.04 ± 0.06	8.16 ± 0.01
Stearic acid (C18:0)	2.58 ± 0.02	2.62 ± 0.02
Oleic acid (C18:1)	4.12 ± 0.01	4.15 ± 0.04
Linoleic acid (C18:2)	0.66 ± 0.04	0.31 ± 0.03
Saturated Fatty acids	94.79	95.53
Monounsaturated Fatty acids	4.12	4.15
Polyunsaturated Fatty acids	0.66	0.31

[a] RBD CO = Refined, bleached and deodorized Coconut oil Data represents means ± standard deviation (n = 3).

3.2. Principal component analysis

PCA, which is an exploratory approach, was applied to evaluate the relationship between PCO and its different adulterants with FCO. The optimized spectral region (3000-2800 cm^{-1} and 1800 to 500 cm^{-1}) was selected for the classification using PCA due to its potential to offer clear separation among adulterated samples. PCA helps in the visualization of the difference between PCO and its different adulterants with FCO. The output of PCA showed separate clusters of PCO and its FCO

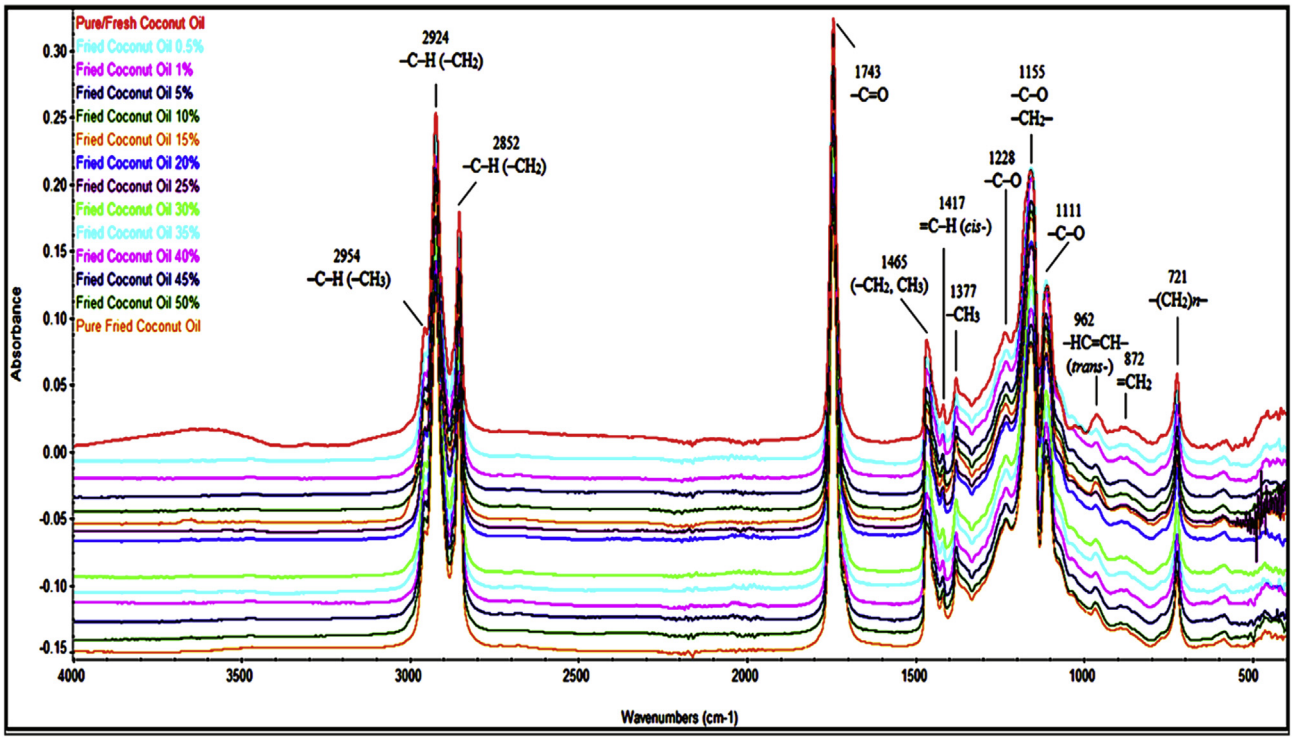

Fig. 1. FTIR spectra of pure coconut oil and different percentage of fried coconut oil depicting major peaks with assigned wavenumbers (cm^{-1}).

adulterants in the resulting 3D score plot with no overlapping of any samples (Fig. 2a). The variance percentages for the first three principal components described 48%, 19%, and 17%, respectively, explaining a total of 94% of the data, indicating the potential of FTIR in the detection of FCO in PCO. A well-defined clustering can be observed in the score plot wherein the PCO samples with the highest adulteration of FCO (50%) are far away from the clusters of PCO samples. The samples which are making groups among themselves are the one having the same percentages of adulteration and therefore have similar characteristics. Moreover, PCA correlation loading spectra for the first three PCs depict the biochemical fingerprint for classification among PCO and FCO adulterants by few specific wavenumbers showing their importance. Both positive and negative score values at different peaks of the PCA loading suggests a significant contribution to the spectrum. PC1 and PC2 depict 48%, and 19% of the explained variance, respectively, was mainly associated with positive and negative score values whereas, PC3 explains 17% of the variance and weights notably only on negative score values. The wavenumbers on positive and negative scale of PC1 are 2954 cm^{-1}, 2924 cm^{-1}, 2852 cm^{-1} which are attributed to stretching vibrations (symmetrical and asymmetrical) of –C–H (–CH_2, –CH_3) groups, 1743 cm^{-1} and 1417 cm^{-1} are associated to stretching of –C═O (ester group) and bending (rocking) of = C–H (*cis*-) group, 1228 cm^{-1} and 1111 cm^{-1} are corresponding to stretching of –C–O group and 872 cm^{-1} and 721 cm^{-1} are associated with bending vibrations of = CH_2 group respectively. In PC2, wavenumber 1155 cm^{-1} on negative scale corresponds to stretching and bending vibration of –C–O and –CH_2– groups, respectively. Whereas on the positive scale, peak at 962 cm^{-1} is attributing to out of plane bending of –HC═CH– (*trans*-) group, which emerges in oils when the level of trans fatty acids increases, which results in the generation of secondary

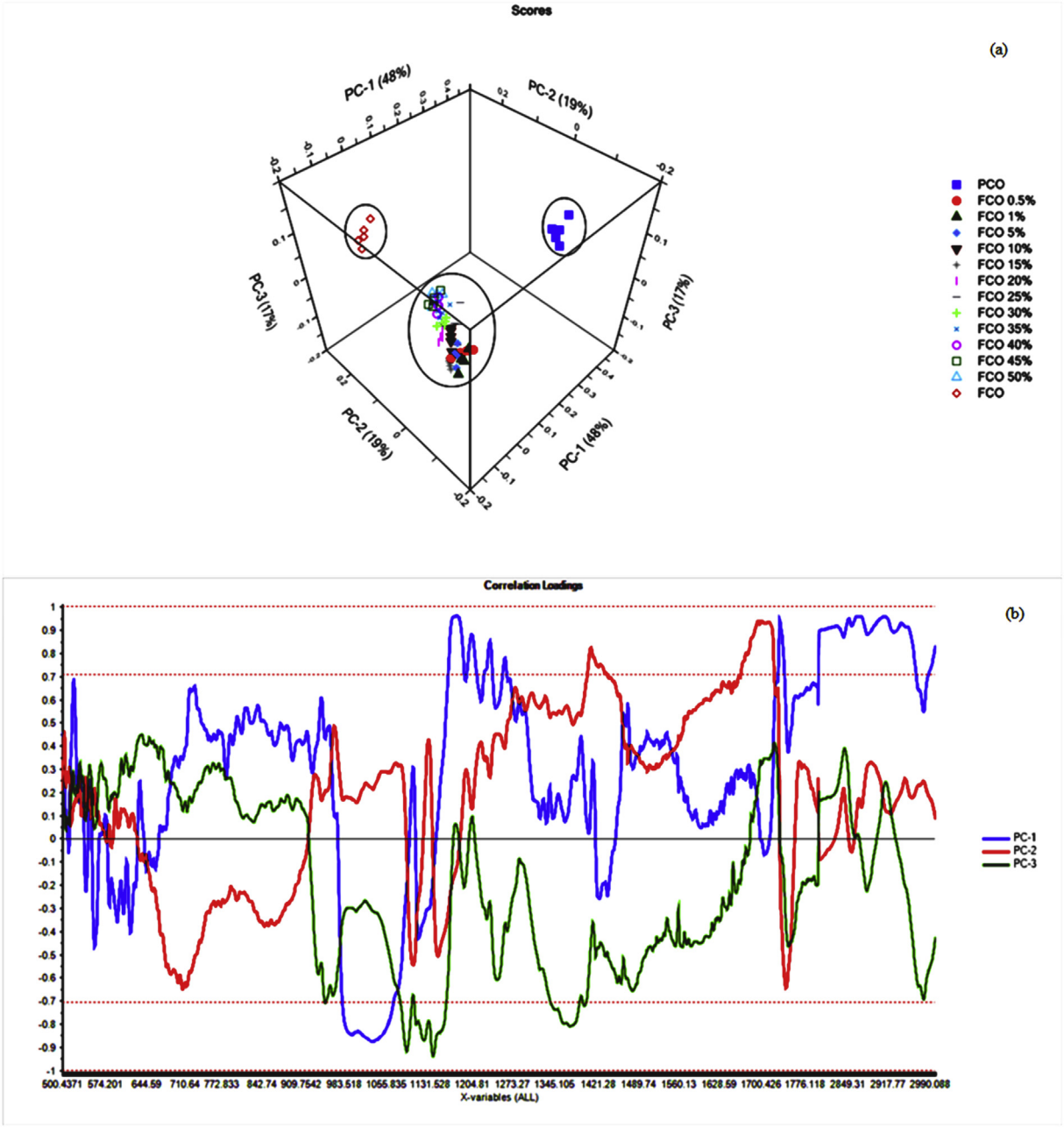

Fig. 2. a) 3D Score plot of pure coconut oil (PCO), PCO/FCO blends and fried coconut oil (FCO) from PCA analysis of FTIR spectra for the combined informative region (3000-2800 cm^{-1} and 1800-500 cm^{-1}) **b)** PCA loading spectra of first three principal components for the combined informative region (3000-2800 cm^{-1} and 1800-500 cm^{-1}).

oxidation products like aldehydes and ketones. Moreover, wavenumbers associated with PC3 loadings are on the negative scale and associated with bending of –C–H (–CH_2, CH_3) groups at 1465 cm^{-1} and bending of –C–H (–CH_3) group at 1377 cm^{-1} respectively (Fig. 2b) (Amit et al., 2020). Therefore, analysis of PC1, PC2, PC3 loadings, and FTIR spectra shows significant signals of different vibrations of assigned functional groups at specific wavenumbers. These wavenumbers contribute to the major peaks in the informative region of the spectra, differentiating the PCO and FCO adulterants (Table 2).

3.3. Linear discriminant analysis

To attain good performance in discrimination of PCO and FCO adulterants, LDA was applied to sample subsets of PCO 100%, FCO 0.5%, and FCO 1% using 13 wavenumbers extracted from the PCA correlation loading spectra. The LDA was computed using a subset of the calibration set for every class having five replications. The output of LDA resulted in 100% accurate classification of initial classes and 100% correctly when cross-validated using leave-one-out validation method, as shown in the confusion matrix (Table 4). To illustrate our results, all group scatter plot showing a discriminant score for the classification of PCO and FCO is shown in Fig. 3. The excellent discrimination was attained in the space for the first two discriminant scores (DF1 and DF2), accounting for 96.1% and 3.9%, respectively. Clear discrimination between all four classes can be observed. From the results, it has been found that samples of FCO 0.5% class correspond to the minimum concentration of FCO used. Hence, the lowest detectable limit of FCO in PCO was 0.5% v/v. This detected concentration is not the constraint of the experimental procedure pursued; instead, it is because of this lowest concentration of FCO adulteration used in our work.

3.4. Multivariate regression modelling

The two most common multivariate methods PCR and PLS-R were used to build regression models on different informative, optimized regions selected from the FTIR spectra. Both methods use independent predictor variables from lower dimensions, which can result in reducing the number of dimensions. Independent variables may be enormously collinear in the case of many linear regression as well as prediction equations. Both methods solve the problem of co-linearity, but PLS-R is more reliable because it uses a lesser number of factors when compared to PCR (Yue, Feng, Yang, & Li, 2018). Above mentioned models comprised of two parts noted as calibration and prediction. During calibration model construction, spectral data of calibration set was utilized to build a regression equation between spectral data (self-reliant variable 'Y') and the various percentages of PCO and FCO blends (reliant variable 'X'). In the prediction part, an external dataset (which was not utilized in the above model construction) is fed into this built model to calculate the concentration of these known samples (Wu, Li, & Tu, 2015). The relation between the number of factors and RMSECV by using the Leave-One-Out approach leads to the determination of the optimum number of factors for the constructed models (Rohman, Che Man, Ismail, & Hashim, 2017). This process plays a critical role in reducing the RMSECV value to the minimum. Moreover, the gap between RMSEC and RMSECV values should be least at the optimum number of factors. Because an increase in the number of factors leads to over-fitting hence low predictive power, while fewer factors lead to under-fitting of the model, which results in loss of information (Kamruzzaman et al., 2016). The modelling adjustment by selecting the optimum number of factors is made based on the minimum gap (maximum proximity) between RMSEC and RMSECV values (Bro, Rinnan, & Faber, 2005). It has also been seen that instead of RMSEC when RMSECV is used as a bias measure for the model selection, it gives less number of factors. (Gowen, Downey, Esquerre, & O'Donnell, 2011). RMSECV should always be slightly higher than RMSEC. The comparative significance of the built model is estimated by using RMSEC, RMSECV, and R^2 values. The model with greater R^2 value and lesser RMSEC and RMSECV value is comparatively more efficient. Similarly, the predictive ability of the built model is tested by analyzing R^2 and RMSEP values. The tested model with greater R^2 and smaller RMSEP values is considered as a comparatively better predictable model (Rohman et al., 2017).

Different validation parameters were calculated for both the calibration and prediction section of every model built. R^2, RMSE, and RE % were calculated for both the sections, whereas RPD, SEP and BIAS were estimated for the prediction section only. All the measured values, along with the optimum number of factors for the combined and the individual optimized spectra, are depicted in Table 5. For obtaining the lowest concentration of detection, PCR, and PLS-R models were built and distinguished for normal, 1st, and 2nd derivative of the individually optimized and combined spectra (Fig. 4). The most efficient model in terms of accuracy and precision was chosen in terms of the highest R^2, RPD, and the least RE% and RMSE values. The calculated value of FCO adulteration against the predicted value obtained from the spectral analysis of the most efficient model is presented in Fig. 5.

During the comparative analysis of all models, R^2 varied from 0.951 to 0.996 (calibration dataset) and from 0.954 to 0.997 (for external dataset). Similarly, RMSEC and RMSEP varied from 1.001 to 3.756% v/v and 0.832–5.225% v/v respectively (Table 5). The most efficient model was observed for the 1st derivative PLS-R model of 1800-500 cm^{-1} spectrum with best quality parameters for calibration in terms of highest R^2 (0.996) and least RMSEC (1.001% v/v) and RE % (4.703). In the case of model predictability, a low BIAS of 0.026 was obtained, signifying a low addition to the SEP of 0.865 (Fig. 5). Similarly, the quality parameters of prediction presented outstanding accuracy and precision with greatest R^2 and RPD of 0.997 and 20.03 and least RMSEP and RE % of 0.832% and 4.288, respectively (Pereira et al., 2019). Therefore, the PLS-R model for the 1st derivative of the 1800-500 cm^{-1} spectrum can be best utilized for the detection of FCO up to 0.5% v/v blending in PCO.

4. Conclusion

It has been demonstrated for the first time that harmful FCO can be detected in PCO by utilizing ATR-FTIR spectroscopy integrated with multivariate regression modelling. This whole technology is rapid,

Table 4
Confusion matrix for the classification of PCO, FCO and different PCO adulterants with FCO.

Classification Results							
		Oil Samples	Predicted Group Membership				Total
			[a]PCO	[b]FCO 0.5%	FCO 1%	FCO	
Original	Count	PCO	5	0	0	0	5
		FCO 0.5%	0	5	0	0	5
		FCO 1%	0	0	5	0	5
		FCO	0	0	0	5	5
	%	PCO	100	0	0	0	100
		FCO 0.5%	0	100	0	0	100
		FCO 1%	0	0	100	0	100
		FCO	0	0	0	100	100
Cross-validated	Count	PCO	5	0	0	0	5
		FCO 0.5%	0	5	0	0	5
		FCO 1%	0	0	5	0	5
		FCO	0	0	0	5	5
	%	PCO	100	0	0	0	100
		FCO 0.5%	0	100	0	0	100
		FCO 1%	0	0	100	0	100
		FCO	0	0	0	100	100

[a] PCO: Pure and fresh Coconut Oil.
[b] FCO: Fried Coconut Oil.

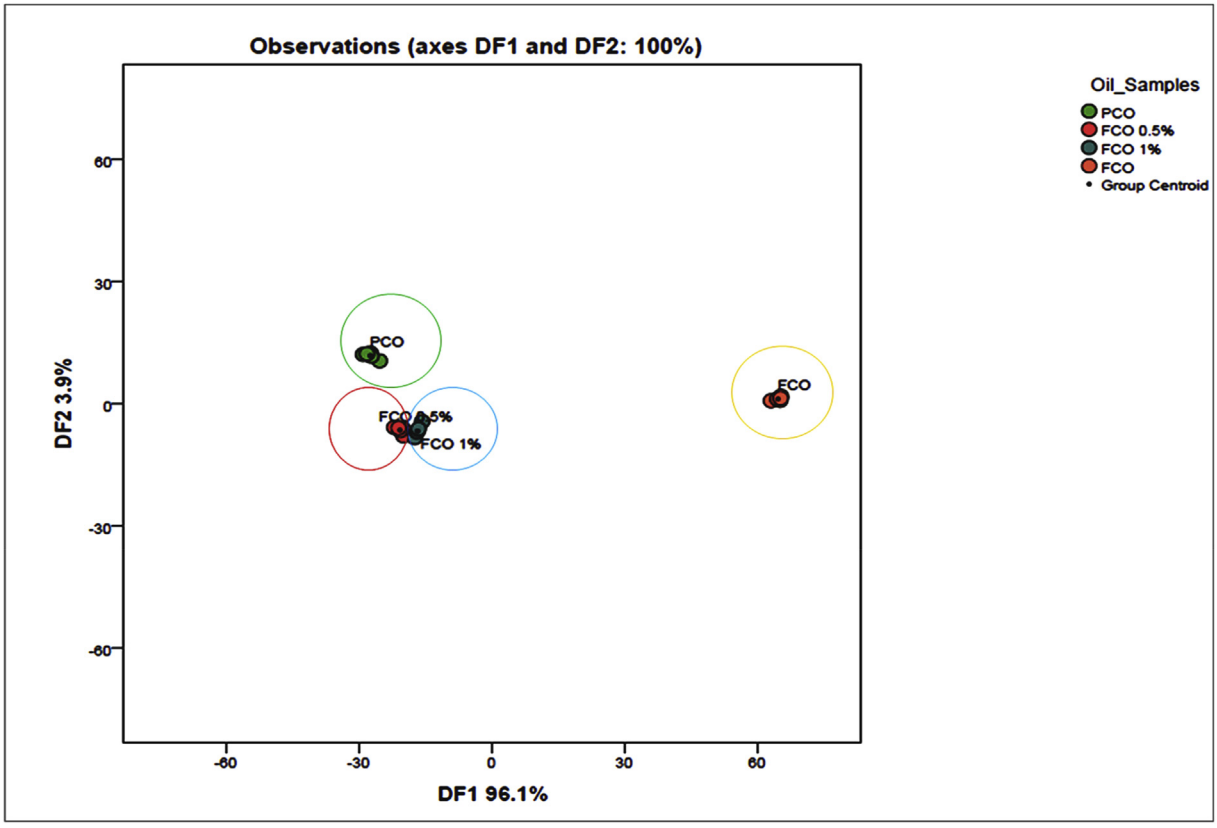

Fig. 3. All groups scatter plot as deduced by discriminant analysis using discriminant function 1 and 2 for FTIR spectral data of PCO, FCO 0.5%, FCO 1% and FCO.

Table 5
PCR and PLS-R models for (a) Combined informative region (3000-2800 cm^{-1} and 1800-500 cm^{-1}) (b) 3000-2800 cm^{-1} (c) 1800-500 cm^{-1}.

Model	Spectra	Factor	Calibration	[a]R^2 Validation	Prediction	[b]RMSEC	RMSE [c]RMSECV	[d]RMSEP	[g]RE % (Cal)	[h]RPD	RE% (Pred)	BIAS	[i]SEP
(a) Combined informative spectral region (3000- 2800 cm^{-1} and 1800-500 cm^{-1})													
[e]PCR	Normal	6	0.982	0.974	0.988	2.247	2.685	1.809	7.047	9.29	6.323	0.113	1.880
	1st derivative	3	0.985	0.905	0.905	1.938	2.080	5.225	6.545	9.24	10.747	−4.969	1.931
	2nd derivative	6	0.966	0.959	0.983	3.108	3.470	2.177	8.288	7.850	6.937	−0.028	2.266
[f]PLS-R	Normal	4	0.991	0.988	0.993	1.595	1.826	1.332	5.937	12.84	5.426	0.020	1.370
	1st derivative	3	0.992	0.990	0.904	1.493	1.673	5.247	5.744	11.28	10.769	−5.021	1.587
	2nd derivative	5	0.980	0.970	0.991	2.383	2.969	1.527	7.257	11.15	5.809	−0.058	1.589
(b) 3000- 2800 cm^{-1}													
PCR	Normal	7	0.986	0.982	0.991	1.949	2.260	1.558	6.563	10.88	5.868	0.146	1.614
	1st derivative	5	0.968	0.964	0.977	3.009	3.265	2.563	8.155	6.750	7.527	−0.571	2.601
	2nd derivative	5	0.951	0.941	0.954	3.756	4.154	3.618	9.111	4.530	8.942	−0.775	3.678
PLS-R	Normal	6	0.983	0.977	0.981	2.182	2.561	2.323	6.945	7.220	7.165	0.212	2.408
	1st derivative	6	0.993	0.981	0.995	1.340	2.350	1.194	5.442	14.47	5.137	−0.266	1.211
	2nd derivative	5	0.969	0.953	0.973	2.947	3.706	2.767	8.071	6.120	7.820	−0.739	2.775
(c) 1800-500 cm^{-1}													
PCR	Normal	5	0.993	0.991	0.995	1.327	1.599	1.166	5.416	14.54	5.076	0.089	1.210
	1st derivative	4	0.985	0.983	0.987	2.023	2.188	1.863	6.687	8.935	6.147	0.099	1.936
	2nd derivative	5	0.963	0.958	0.978	3.226	3.514	2.505	8.444	6.780	7.441	−0.033	2.607
PLS-R	Normal	4	0.990	0.988	0.995	1.612	1.818	1.169	5.699	14.63	5.083	0.118	1.211
	1st derivative	5	0.996	0.993	0.997	1.001	1.399	0.832	4.703	20.03	4.288	0.026	0.865
	2nd derivative	6	0.995	0.987	0.996	1.146	1.913	0.935	5.033	17.70	4.546	−0.044	0.937

[a] R^2: Coefficient of determination.
[b] RMSEC: Root mean square error of calibration.
[c] RMSECV; Root mean square error of cross validation.
[d] RMSEP; Root mean square error of prediction.
[e] PCR: Principal component regression.
[f] PLS-R: Partial least squares regression.
[g] RE%: Relative Prediction Error.
[h] RPD: Residual Predictive Deviation.
[i] SEP: Standard Error of Prediction.

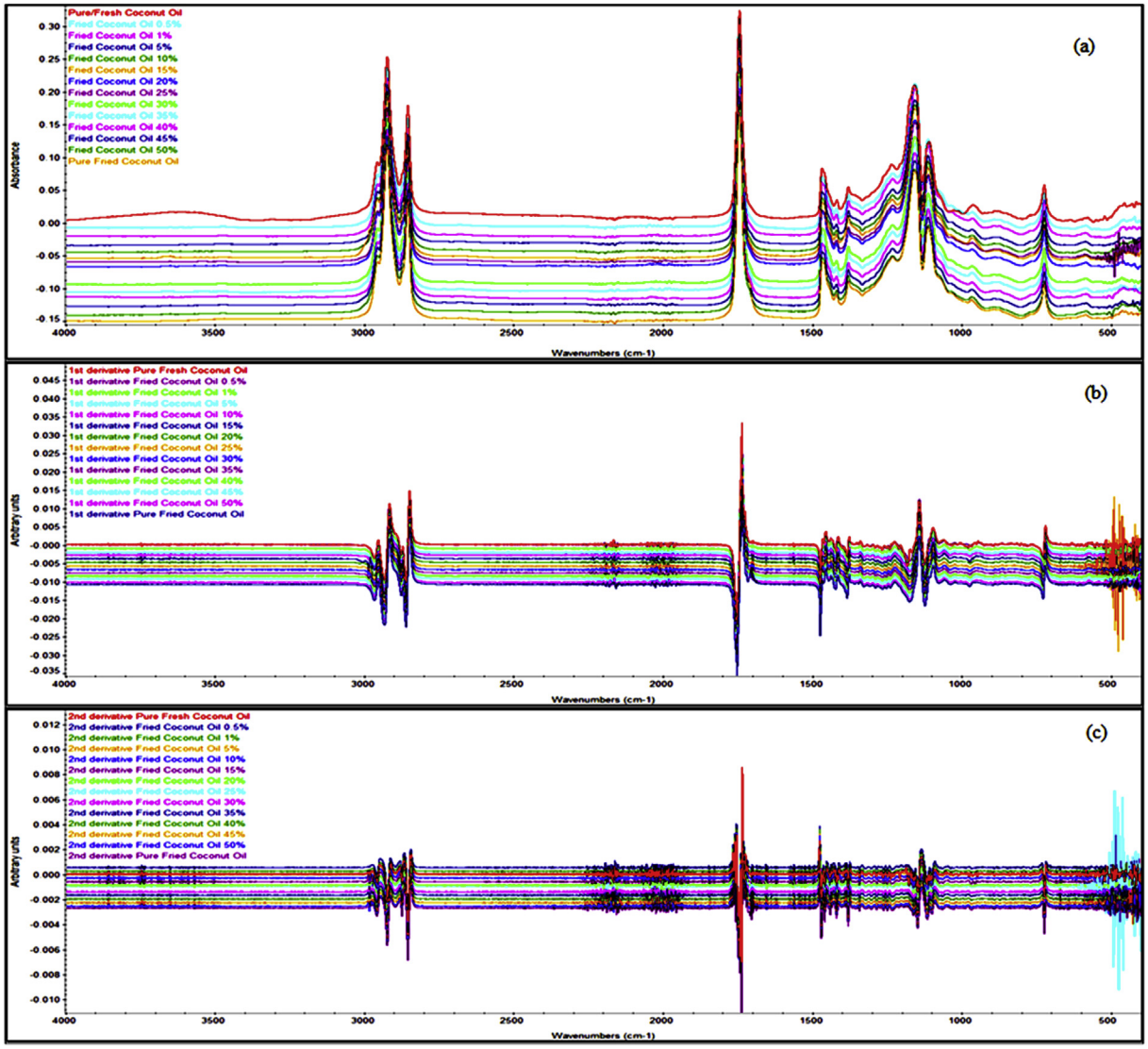

Fig. 4. Overlay FTIR spectra of PCO and its various FCO blends in the region of 4000-400 $cm^{-1}$for (a) normal, (b) first derivative (c) second derivative respectively.

requires no extra sample preparation, and does not use noxious chemicals and reagents. PCA and LDA successfully classified and differentiated FCO blends up to 0.5% v/v. For quantification, regression models were established on the combined optimized spectra and the separate optimized spectra of the calibration data matrix. The best regression model was obtained from the 1st derivative data of the 1800-500 cm^{-1} region with the maximum R^2 of 0.997 and the minimum RMSEP of 0.832% v/v. The efficiency of the built models was tested by utilizing test data set that produced little RE % and large RPD (more than 6.5), concluding in immense accuracy and precision. Hence, the lowest detectable limit of FCO in PCO was 0.5% v/v. This detected concentration is not the constraint of the experimental procedure pursued; instead, it is because of this lowest concentration of FCO adulteration used. In our study, we have detected adulteration of PCO with different concentration of FCO at same degree of frying while adulteration detection of FCO at different frying degrees is altogether a different adulteration issue, which is not addressed in our case. Therefore, the mid-infrared FTIR integrated with regression modelling can be employed as an exemplary approach for the detection of FCO blending in PCO. The findings from our study can provide valuable information to the oil-producing industries and the regulatory authorities to build standard guidelines for the detection of FCO adulteration.

CRediT authorship contribution statement

Amit: Conceptualization, Software, Validation, Formal analysis, Writing - original draft. **Rahul Jamwal:** Software, Methodology, Validation, Formal analysis, Writing - review & editing. **Shivani Kumari:** Investigation, Data curation. **Simon Kelly:** Formal analysis. **Andrew Cannavan:** Formal analysis. **Dileep Kumar Singh:** Supervision, Project administration.

Declaration of competing interest

The authors have no conflict of interest.

Acknowledgment

We are profoundly thankful for International Atomic Energy Agency, Vienna, Austria, for its compassionate support for funding through a research project named “Field-deployable analytical methods to access the authenticity, safety, and quality of food in India” (IAEA Project contract number - 22125). We are grateful to the University of Delhi, Delhi, for helping with the infrastructure needed for the work. Lastly, we would like to thank the Council of Scientific and Industrial Research (CSIR) Government of India, for providing fellowship to the

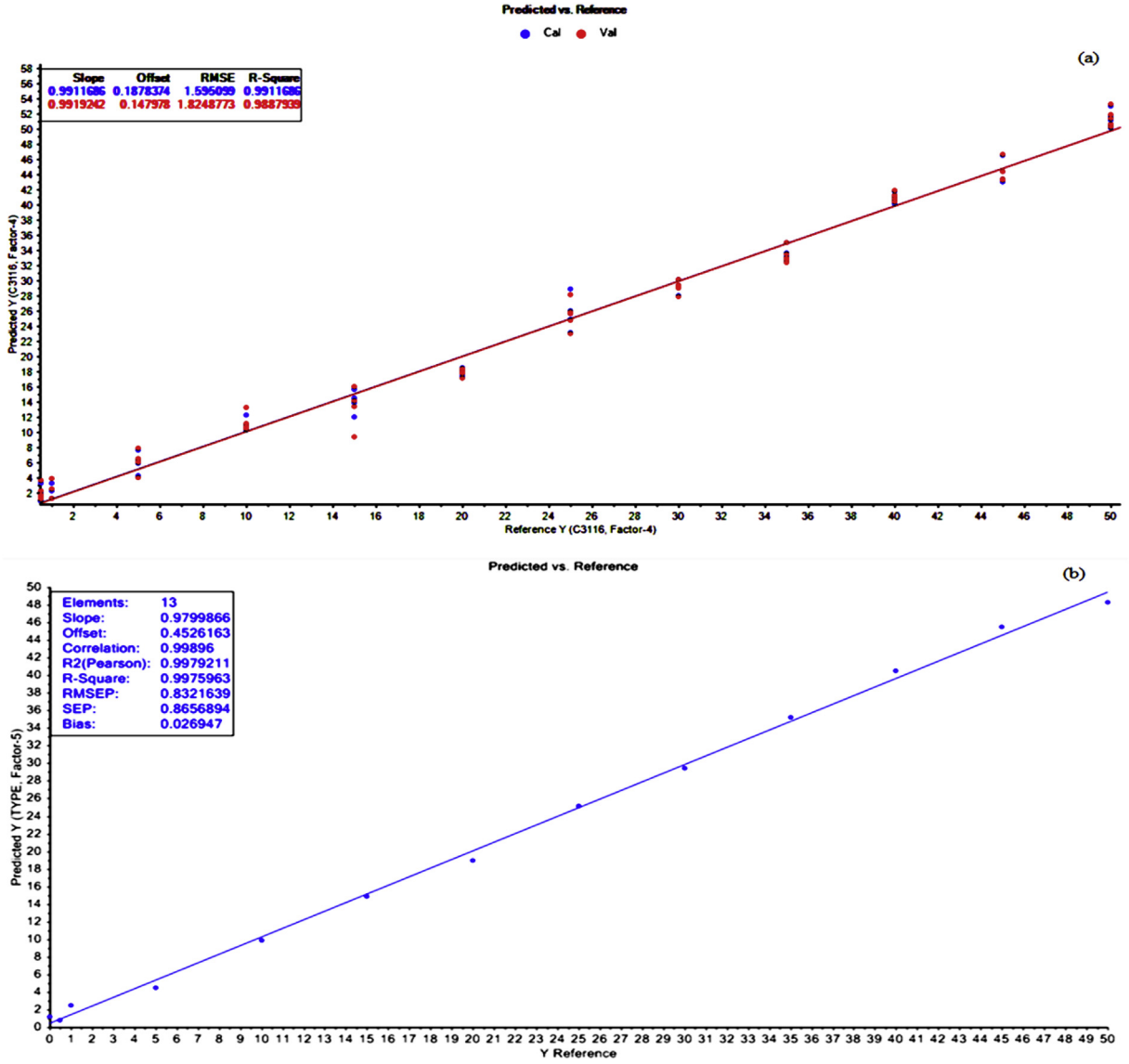

Fig. 5. a) Partial least squares regression (PLS-R) calibration model of 1st derivative of separate optimized region (1800 cm^{-1} to 500 cm^{-1}) for relationship between actual (Reference Y) versus FTIR predicted adulteration level of FCO in PCO (Predicted Y) **b)** Partial least squares regression (PLS-R) prediction for 1st derivative of separate optimized region (1800 cm^{-1} to 500 cm^{-1}).

first author.

References

Amit, Jamwal, R., Kumari, S., Dhaulaniya, A. S., Balan, B., & Singh, D. K. (2020). Application of ATR-FTIR spectroscopy along with regression modelling for the detection of adulteration of virgin coconut oil with paraffin oil. *Lebensmittel-Wissenschaft und -Technologie- Food Science and Technology, 118*, 108754.

Andrade, J., Pereira, C. G., de Almeida Junior, J. C., Viana, C. C. R., de Oliveira Neves, L. N., da Silva, P. H. F., et al. (2019). FTIR-ATR determination of protein content to evaluate whey protein concentrate adulteration. *Lebensmittel-Wissenschaft und -Technologie- Food Science and Technology, 99*, 166–172.

Bro, R., Rinnan, Å., & Faber, N. K. M. (2005). Standard error of prediction for multilinear PLS: 2. Practical implementation in fluorescence spectroscopy. *Chemometrics and Intelligent Laboratory Systems, 75*(1), 69–76.

Brühl, L. (2014). Fatty acid alterations in oils and fats during heating and frying. *European Journal of Lipid Science and Technology, 116*(6), 707–715.

Che Man, Y. B., & Tan, C. P. (1999). Effects of natural and synthetic antioxidants on changes in refined, bleached, and deodorized palm olein during deep-fat frying of potato chips. *Journal of the American Oil Chemists' Society, 76*(3), 331–339.

Endo, Y. (2018). Analytical methods to evaluate the quality of edible fats and oils: The JOCS standard methods for analysis of fats, oils and related materials (2013) and advanced methods. *Journal of Oleo Science, 67*(1), 1–10.

Ghani, N. A. A., Channip, A. A., Chok Hwee Hwa, P., Ja'afar, F., Yasin, H. M., & Usman, A. (2018). Physicochemical properties, antioxidant capacities, and metal contents of virgin coconut oil produced by wet and dry processes. *Food Science & Nutrition, 6*(5), 1298–1306.

Ghobadi, S., Akhlaghi, M., Shams, S., & Mazloomi, S. M. (2018). Acid and peroxide values and total polar compounds of frying oils in fast food restaurants of Shiraz, Southern Iran. *International Journal of Nutrition Sciences, 3*(1), 25–30.

Gowen, A. A., Downey, G., Esquerre, C., & O'Donnell, C. P. (2011). Preventing over-fitting in PLS calibration models of near-infrared (NIR) spectroscopy data using regression coefficients. *Journal of Chemometrics, 25*(7), 375–381.

Guillaume, C., De Alzaa, F., & Ravetti, L. (2018). Evaluation of chemical and physical changes in different commercial oils during heating. *Acta Scientific Nutritional Health, 2*, 2–11.

Hammouda, I. B., Zribi, A., Mansour, A. B., Matthäus, B., & Bouaziz, M. (2017). Effect of deep-frying on 3-MCPD esters and glycidyl esters contents and quality control of refined olive pomace oil blended with refined palm oil. *European Food Research and Technology, 243*(7), 1219–1227.

Hamsi, M. A., Othman, F., Das, S., Kamisah, Y., Thent, Z. C., Qodriyah, H. M. S., et al. (2015). Effect of consumption of fresh and heated virgin coconut oil on the blood pressure and inflammatory biomarkers: An experimental study in Sprague Dawley rats. *Alexandria Journal of Medicine, 51*(1), 53–63.

Henna Lu, F. S., & Tan, P. P. (2009). A comparative study of storage stability in virgin coconut oil and extra virgin olive oil upon thermal treatment. *International Food Research Journal, 16*, 343–354.

Jamwal, R., Kumari, S., Balan, B., Dhaulaniya, A. S., Kelly, S., Cannavan, A., et al. (2020). Attenuated total Reflectance–Fourier transform infrared (ATR–FTIR) spectroscopy coupled with chemometrics for rapid detection of argemone oil adulteration in mustard oil. Lebensmittel-Wissenschaft und -Technologie. *Food Science and*

Technology, 120, 108945.
Jović, O., Smolić, T., Primožič, I., & Hrenar, T. (2016). Spectroscopic and chemometric analysis of binary and ternary edible oil mixtures: Qualitative and quantitative study. *Analytical Chemistry, 88*(8), 4516–4524.
Kamruzzaman, M., Makino, Y., & Oshita, S. (2016). Rapid and non-destructive detection of chicken adulteration in minced beef using visible near-infrared hyperspectral imaging and machine learning. *Journal of Food Engineering, 170*, 8–15.
Koh, S. P., & Long, K. (2012). Oxidative stability study of virgin coconut oil during deep frying. *Journal of Tropical Agriculture and Food Science, 40*(1), 35–44.
Lim, S. Y., Abdul Mutalib, M. S., Khaza'ai, H., & Chang, S. K. (2018). Detection of fresh palm oil adulteration with recycled cooking oil using fatty acid composition and FTIR spectral analysis. *International Journal of Food Properties, 21*(1), 2428–2451.
Marina, A. M., Man, Y. C., & Amin, I. (2009). Virgin coconut oil: Emerging functional food oil. *Trends in Food Science & Technology, 20*(10), 481–487.
Moigradean, D., Poiana, M. A., & Gogoasa, I. (2012). Quality characteristics and oxidative stability of coconut oil during storage. *Journal of Agroalimentary Processes and Technologies, 18*(4), 272–276.
Pereira, C. G., Leite, A. I. N., Andrade, J., Bell, M. J. V., & Anjos, V. (2019). Evaluation of butter oil adulteration with soybean oil by FT-MIR and FT-NIR spectroscopies and multivariate analyses. *Lebensmittel-Wissenschaft und -Technologie- Food Science and Technology, 107*, 1–8.
Rohman, A., Che Man, Y. B., Ismail, A., & Hashim, P. (2017). FTIR spectroscopy coupled with chemometrics of multivariate calibration and discriminant analysis for authentication of extra virgin olive oil. *International Journal of Food Properties, 20*(sup1), S1173–S1181.
Rohman, A., Setyaningrum, D. L., & Riyanto, S. (2014). FTIR spectroscopy combined with partial least square for analysis of red fruit oil in ternary mixture system. *International Journal of Spectroscopy, 2014*, 5 785914.
Savitzky, A., & Golay, M. J. (1964). Smoothing and differentiation of data by simplified least squares procedures. *Analytical Chemistry, 36*(8), 1627–1639.
Sunisa, W., Worapong, U., Sunisa, S., Saowaluck, J., & Saowakon, W. (2011). Quality changes of chicken frying oil as affected of frying conditions. *International Food Research Journal, 18*(2).
Varmuza, K., & Filzmoser, P. (2016). *Introduction to multivariate statistical analysis in chemometrics.* CRC press.
Vasconcelos, M., Coelho, L., Barros, A., & de Almeida, J. M. M. M. (2015). Study of adulteration of extra virgin olive oil with peanut oil using FTIR spectroscopy and chemometrics. *Cogent Food & Agriculture, 1*(1), 1018695.
Wójcicki, K., Khmelinskii, I., Sikorski, M., & Sikorska, E. (2015). Near and mid infrared spectroscopy and multivariate data analysis in studies of oxidation of edible oils. *Food Chemistry, 187*, 416–423.
Wu, Z., Li, H., & Tu, D. (2015). Application of Fourier Transform Infrared (FT-IR) Spectroscopy combined with chemometrics for analysis of rapeseed oil adulterated with refining and purificating waste cooking oil. *Food Analytical Methods, 8*(10), 2581–2587.
Yue, J., Feng, H., Yang, G., & Li, Z. (2018). A comparison of regression techniques for estimation of above-ground winter wheat biomass using near-surface spectroscopy. *Remote Sensing, 10*(1), 66.
Zhang, X., Saha, A., & Vishwanathan, S. V. N. (2012). Smoothing multivariate performance measures. *Journal of Machine Learning Research, 13*, 3623–3680.
Zribi, A., Jabeur, H., Flamini, G., & Bouaziz, M. (2016). Quality assessment of refined oil blends during repeated deep frying monitored by SPME–GC–EIMS, GC and chemometrics. *International Journal of Food Science and Technology, 51*(7), 1594–1603.